Rapid Blood T_1 Calibration for Arterial Spin Labelling

M. Varela[1], J. V. Hajnal[1], E. T. Petersen[2,3], X. Golay[2,4], and D. J. Larkman[1]

[1]Imaging Sciences Department, MRC Clinical Sciences Centre, Robert Steiner MRI Unit, Hammersmith Hospital, Imperial College London, London, United Kingdom, [2]Department of Neuroradiology, National Neuroscience Institute, Singapore, [3]CFIN, Department of Neuroradiology, Aarhus University Hospital, Aarhus, Denmark, [4]Laboratory of Molecular Imaging, Singapore Bioimaging Consortium, Singapore

INTRODUCTION The longitudinal relaxation time, T_1, of arterial blood is a critical parameter in perfusion quantification using Arterial Spin Labelling (ASL): the use of inaccurate blood T_1, values leads directly to incorrect cerebral blood flow (CBF) estimates [1]. Previous studies suggest that blood T_1, T_{1b}, is strongly dependent on its hematocrit (Hct), changing as much as 10% within the normal adult range (38-46%) [2]. This implies that using standard literature values for blood T_1 in population groups or patients with a hematocrit outside the normal range can cause gross errors in CBF estimation and limit the utility of ASL. Neonates, a group for which cerebral perfusion measurements could constitute a valuable diagnostic tool [3], are likely to fall into this category, since their Hct is generally higher and more variable than that of adults (typically 44-59%) [4].

In this work we present a method for rapid measurement of blood T_1, which can be appended to ASL studies to give direct values of blood T_1 on a subject-by-subject basis and show preliminary results obtained in 5 adults and 2 neonates at 3 T.

METHODS Sequence The sequence performs repeated slice selective 90° excitation pulses with single-shot EPI readouts following a global adiabatic inversion. An optional tissue saturation pulse could also be added after the inversion. The timing between readouts was chosen so that the blood in large vessels contained within the slice would be completely refreshed between each acquisition. Blood therefore follows a standard inversion recovery curve with an effective infinite TR. Static tissue, on the other hand, is subjected to a large flip angle Look-Locker sequence [5], quickly reaching a low signal steady-state. When added, the saturation pulse after the inversion decreased the static tissue signal further.

Data Acquisition This approach was implemented on a 3T Philips Achieva scanner using an 8-channel phased-array head coil and tested on a phantom with flowing and static compartments. In vivo data was acquired in 5 adults (ages 25-38 years) and 2 neonates (ages 7 and 25 days). The imaging slice was positioned perpendicular to the posterior sagittal sinus and intersecting other vessels, whilst avoiding regions of high magnetic susceptibility artefact. The resolution was typically 1.56x1.56 - 1.25x1.25 mm^2 and slice thickness 2 mm. TE was 65 ms and time between excitation pulses typically 115 ms with 25 EPI readouts performed in succession after each inversion. 20 averages were obtained with 6-10 s between successive inversion pulses, in a total scan time of less than 3 min. All the adults had the sequence repeated in a different geometry to assess the reproducibility of the blood T_1 measurements. In one of the adults the measurement was repeated with and without the static tissue saturation pulse. All images were inspected to check for significant movement.

Data Analysis Complex images were used in this analysis to avoid errors due to noise rectification where the signal is close to zero and to allow the use of a model where a static tissue term could easily be incorporated. First, all averages were globally phase corrected to account for scanner dependent phase drift before computation of the complex mean was performed. Following this, an individual phase correction was applied to each voxel and all time points in the series to make the blood signal recovery curve pure real. Data from the first two time points was rejected, given that static tissue had not yet reached a steady-state by then. Voxels with a high percentage of blood were identified by detecting recovery curves with zero crossing later than 700 ms and final recovered signal higher than twice the mean signal. This was followed by visual inspection and rejection of voxels with corrupted time courses. The time evolution of the signal in the remaining voxels ($S_i(t)$) was simultaneously fitted, using a non-linear least squares algorithm, to a mixed tissue inversion recovery model. Free parameters were: equilibrium magnetization for blood (S_{0bi}); real part of the saturated magnetisation for static tissue (S_{0ti}) and T_{1b}. $S_i(t) = S_{0bi}(1-2*\exp(-t/T_{1b}))+S_{oti}$ (1) All these parameters were allowed to vary on a voxel-by-voxel basis except T_{1b}, which was global.

RESULTS It was found that the full mixture model, (1), produced unstable results, giving inconsistent values for T_{1b}. However, setting S_{0t} = 0 in (1), while allowing S_{0b} to vary for each pixel produced reliable results for most blood containing pixels (Fig. 1) with the remainder easily rejected due to systematic fitting failures (χ^2>4*data error^2). Most of the selected voxels belong to the sagittal sinus, with some contribution from peripheral vessels, meaning that the T_{1b} values obtained refer to venous blood. Values for the T_1 of doped water measured in the phantom using our sequence and method (T_1=533 ± 21 ms) were in good agreement with independent inversion recovery measurements in the absence of flow (T_1=559 ± 10 ms), thus confirming the validity of the MR sequence and analysis method. It was found that the use of the tissue saturation pulse helped suppress tissue signal in the first few data points, but as these were subsequently rejected, had little impact on the final results. The values obtained for T_{1b} are listed in table 1. The quoted uncertainty (95% confidence interval) is relative to the least-squares fitting process and does not include the uncertainty associated with the outlier rejection criteria. This results in the quoted error in table 1 being an underestimate of the error in the whole method.

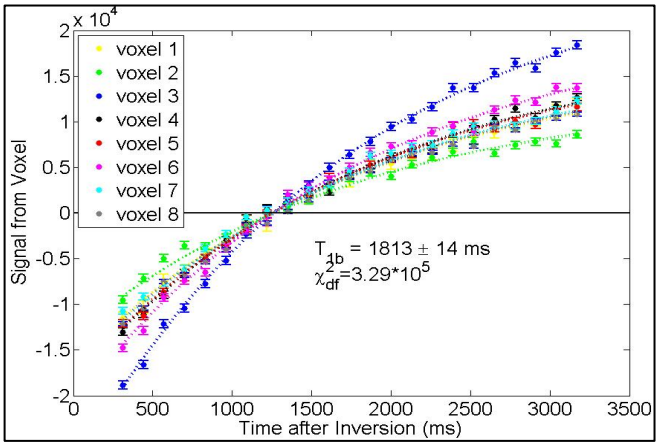

Fig. 1 *- Time evolution of the signal in the selected voxels and corresponding fits to the model for neonate 2. The error bars in the graph are the standard deviation of the imaginary part of the data.*

	Blood T_1 (ms) – 1st trial	Blood T_1 (ms) – 2nd trial
Adult 1	1707 ± 6 (18 voxels)	1741 ± 10 (7 voxels)
Adult 2	1583 ± 12 (15 voxels)	1547 ± 24 (10 voxels)
Adult 3	1616 ± 16 (6 voxels)	1635 ± 14 (16 voxels)
Adult 4	1544 ± 10 (14 voxels)	1584 ± 18 (10 voxels)
Adult 5	1588 ± 14 (6 voxels)	1562 ± 24 (7 voxels)
Neonate 1 (Hct=51%)	1582 ± 20 (8 voxels)	
Neonate 2 (Hct=39%)	1813 ± 14 (8 voxels)	

Table 1 *– T_{1b} values obtained for 5 adults (in 2 trials) and 2 neonates.*

CONCLUSIONS We have presented a method capable of measuring the T_1 of blood prior to an ASL study with a small time penalty and shown that it gives values for blood T_1 in adults that are reproducible and in good agreement with existing literature [2]. A key observation is that partial voluming of blood and static tissue can be almost universally accounted for by a varying blood fraction on a pixel-by-pixel basis - no separate signal contribution is needed from tissue as the Look-Locker readout reduces this to a negligible amount. We have also shown that this method can be used in neonates, with results suggesting that the T_{1blood} for this population, which has a wider range of Hct values, varies more than in adults, although this is clearly a limited study at this stage. Future work will focus on obtaining T_{1b} for pure arterial blood, as well as automating blood voxel selection criteria. Following this, we intend to apply the T_1 direct measurement as part of an ASL study to improve the reproducibility and accuracy of CBF measurements, particularly in neonates.

ACKNOWLEDGEMENTS The Portuguese Foundation for Science and Technology for funding. **REFERENCES** [1] Buxton, R et al. (1998) *Magn Reson Med* 40, 383–396 [2] Lu, H et al. (2004) *J Magn Reson Imaging* 52, 679-682 [3] Wang, J, Licht D (2006*) Neuroimag Clin N Am* 16, 149-167 [4] Rampling, M et al. (1989) *Pediatr Res.* 25, 457-60, [5] Look D, Locker D (1970) *Rev Sci Instrum* 41, 250 –251